J Nanostruct 15(4): 1400-1409, Autumn 2025

RESEARCH PAPER

Enhanced Optical Properties of PAN-PEG Polymer with TiO_2 Nanoparticles for Biological Applications

Lamis Faaz Nassir [1], Shaymaa Al- Rubaye [1], and Ahmed Shaker Hussein [2]*

[1] *Hammurabi College of Medicine, University of Babylon, Iraq*

[2] *College of Dentistry, University of Babylon, Iraq*

ARTICLE INFO

Article History:
Received 02 April 2025
Accepted 17 June 2025
Published 01 October 2025

Keywords:
Absorbance
Nanoparticle
Optical properties
TiO_2

ABSTRACT

This research studied the optical characteristics of PAN-PEG polymeric composite material when titanium oxide (TiO_2) nanoparticles were added to it for improving its use for biological purposes. The XRD and FESEM results confirmed the successful fabrication of a PAN-PEG/TiO_2 nanocomposite, characterized by well-dispersed and highly crystalline anatase TiO_2 nanoparticles. The study examined cooperation of diverse weights of TiO_2 nanoparticles (ranging from 0% to 8%) in PAN-PEG composite. The optical characteristics were evaluated across a spectrum of wavelengths spanning from 220 nm to 800 nm. Results of the experiments highlight that absorbance of PAN-PEG composite increases as concentration of TiO_2 in the mixture increased. The addition of TiO_2 nanoparticle also resulted in a shift in the optical constants and the energy gap of composite. Furthermore, findings of the study revealed potential of PAN-PEG-TiO_2 nanocomposites for gamma ray shielding. Overall, study demonstrates the potential of incorporating TiO_2 nanoparticles into PAN-PEG polymeric composite for improving its optical as well as shielding properties for variety of applications.

How to cite this article
Nassir L., Al- Rubaye S., Hussein A. Enhanced Optical Properties of PAN-PEG Polymer with TiO_2 Nanoparticles for Biological Applications. J Nanostruct, 2025; 15(4):1400-1409. DOI: 10.22052/JNS.2025.04.001

INTRODUCTION

Current research focus on the science and technology applications throughout technical domains. The field of research involves polymer science and technology in different applications including micro-nanoelectronics. Different areas within nanocomposite science include "bactericidal properties, composite reinforcement, barrier properties, cosmetic applications and electro-optical properties [1-4]. Research in this area has included fuel cell electrodes, nanoparticle drug delivery, biomaterials derived from polymers, catalysts attached to polymers, miniemulsion particles, self-assembling polymer films, blends of polymers, and nanocomposites. Nanocomposites exhibit multiple themes which involve bactericidal properties along with composite reinforcement, flame resistance, barrier properties, aesthetic capabilities and electro-optical properties [1, 2, 5, 6]. A special case of composite material is a material constructed such that the interaction between the different materials reinforce one another to create a new substance with properties that exceed the individual ones of either of the ingredients in a given application. Composites, due to their high hardness, high melting point, low density, and high

* *Corresponding Author Email: nur.lamis.nassier@uobabylon.edu.iq*

thermal conductivity, offer promising prospects in various industrial fields [7]. In recent years, polymer-based nanocomposites have introduced as highly adaptable and sophisticated materials. The development of polymer nanocomposites has expanded the range of potential applications for coatings and adhesives. The characteristics of polymer nanocomposite coatings are a result of the change of fillers and the methods employed in their manufacture. The polyacrylonitrile (PAN) is a synthetic resin and a product of the polymerization of acrylonitrile. This material is a well-known category of acrylic resins, however it is a strong and durable thermoplastic shape. It has excellent resistance to solvents and chemicals with moderate combustion speed and little gas permeability. The majority of PAN is manufactured in the form of acrylic and modacrylic fibers, which are widely used as alternatives to wool in the production of apparel and home goods. A semicrystalline organic polymer, PAN, with nitrile's chemical formula of $(C_3H_3N)_n$, has nitrile (CN) functional group as the unit structure. Nitrile functional groups are excellent hydrogen bonding acceptors because of the nitrogen atom's lone pair. Additionally, nitriles may be used to produce very strong attractive connections due to the large dipole moment between the electron-poor carbon atom and the electron-rich nitrogen atom. The high strength and resistance of many organic solvents are induced by the strong intermolecular interaction [8-12]. Optical spectroscopy is often regarded as a highly effective method for elucidating the band structure of materials. Very favorable electron transport and mechanical as well as optical features have made polymer-based nanocomposites interesting for a large number of applications in medical and engineering technology [13]. Optical spectroscopy in the modified state may also be used to investigate electronic band structure of the crystal. In order to study functional materials, it is important to possess a comprehensive understanding of the band gap associated with the material. PAN is considered to be a polymer with exceptional versatility, mostly attributed to its elevated carbon content [14-17]. It is highly biostable because of its carbon-carbon backbone and it is resistant to degradation. The polymerization of acrylonitrile monomer ultimately results in the formation of PAN in either granulated or powdered form. This powder, in its natural state, has very few applications in the manufacturing business. Therefore, in order to form polymer, it needs to be treated with a large number of co-monomers in a different form [18].

MATERIAL AND METHODS

The casting procedure was used to fabricate the polymer blend that consisted of PAN (90% weight) and polyethylene glycol (PEG ,5% weight). Suppressors of nano-composition were made with different weight percentages of titanium oxide (TiO_2) nanoparticles (0, 2, 4, 6 and 8). Measurements of absorbance and transmittance spectra of resulting PAN-PEG-TiO_2 nanocomposites within a wavelength span of 220-800 nm were studied by the UV/1800/ Shimadzu spectrophotometer. The Eq. 1 [19] can be used to calculate the absorption coefficient (α) of PAN-PEG-TiO_2 nanocomposites:

$$\alpha = 2.303A/d \quad (1)$$

where, d is the sample thickness. A is the absorbance of the nanocomposites. Eq. 2 [20] establish the electrical transitions model of amorphous semiconductors.

$$\alpha h\upsilon = B(h\upsilon - Eg)^n \quad (2)$$

For an indirect transition, n is 2, and for an indirect transition, n is 3. Here, C is the constant, hυ is the photon energy, and Eg is the optical energy band gap. The Eq. 3 [20] was employed to determine the extinction coefficient (k) of the PAN-PEG-TiO_2 nanocomposites:

$$K = \alpha\lambda/4\pi \quad (3)$$

When k→0, the Eq. 4 [21] describes the refractive index (n) of the PAN-PEG-TiO_2 nanocomposites:

$$n = (1+R^{1/2})/(1-R^{1/2}) \quad (4)$$

where, R is the reflectance. The actual (1) and imaginary (2) components of the dielectric constant of the PAN-PEG-TiO_2 nanocomposites were ascertained using Eq. 5 and 6 [22]:

$$\varepsilon_1 = n^2 - k^2 \quad (5)$$

$$\varepsilon_2 = 2nk \quad (6)$$

RESULTS AND DISCUSSION

XRD analysis was carried out for better understanding the crystalinity of materials. The XRD pattern of TiO_2 (Fig. 1a) clearly demonstrates the presence of pure anatase phase TiO_2 nanoparticles with excellent crystalline quality. The dominant peak at 2θ ≈ 25° corresponds to the (101) crystallographic plane of anatase, which is the most characteristic peak for this phase. Additional well-defined peaks at 37-38°, 48°, 54-55°, 62°, 69°, and 75° correspond to the phase purity with no detectable rutile contamination. The intense peaks with low background noise indicate high crystallinity and minimal amorphous content, which are crucial for enhanced optical properties in biological applications. The the pure anatase phase is particularly advantageous for PAN-PEG composite system due to its superior photocatalytic activity, better biocompatibility, and

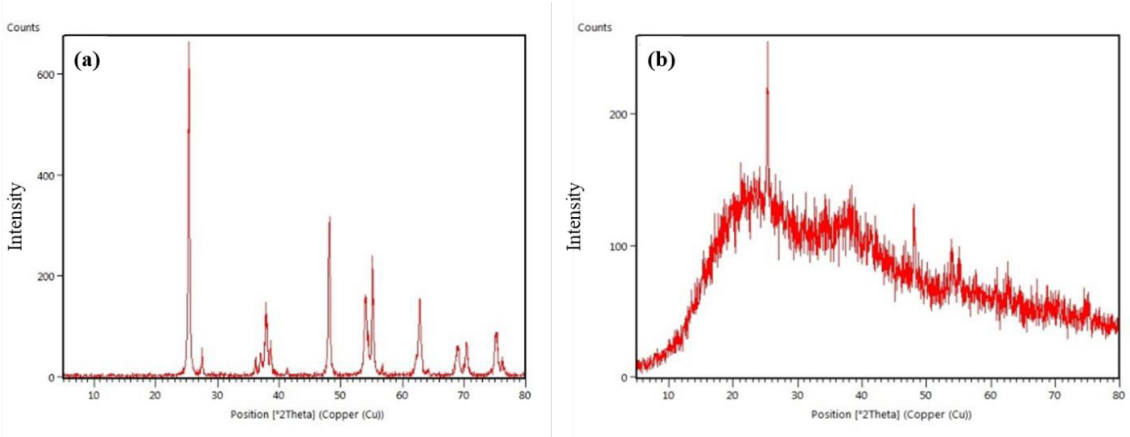

Fig. 1. XRD patterns of (a) TiO_2 nanoparticles and (b) PAN-PEG/TiO_2 nanocomposite.

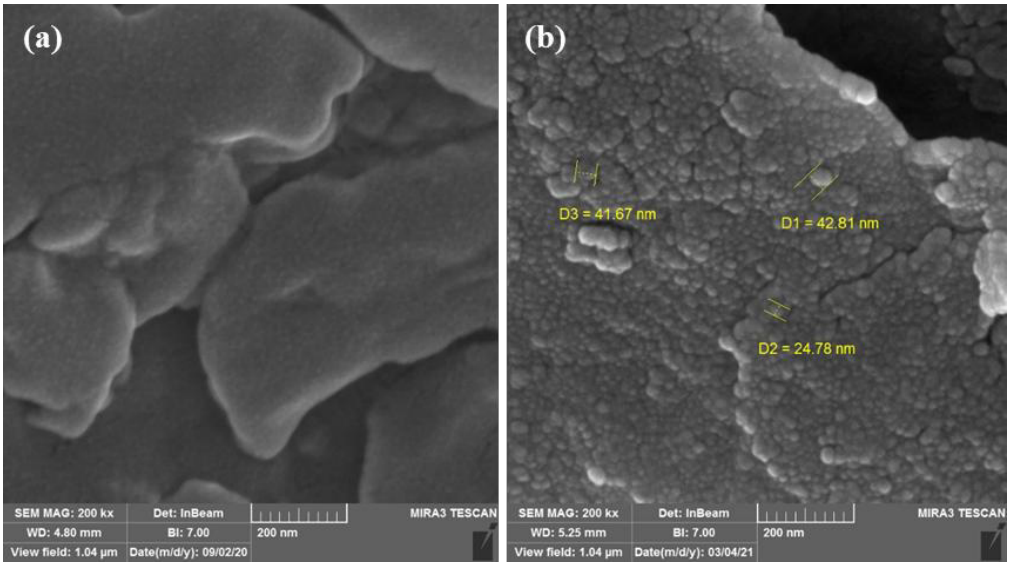

Fig. 2. FF-ESEM images of (a) PAN-PEG and (b) PAN-PEG/TiO_2 nanocomposite.

enhanced UV absorption properties as compared to other TiO_2 phases, making it ideal for biological sensing and antimicrobial applications. The XRD pattern of resulting PAN-PEG/TiO_2 nanocomposite

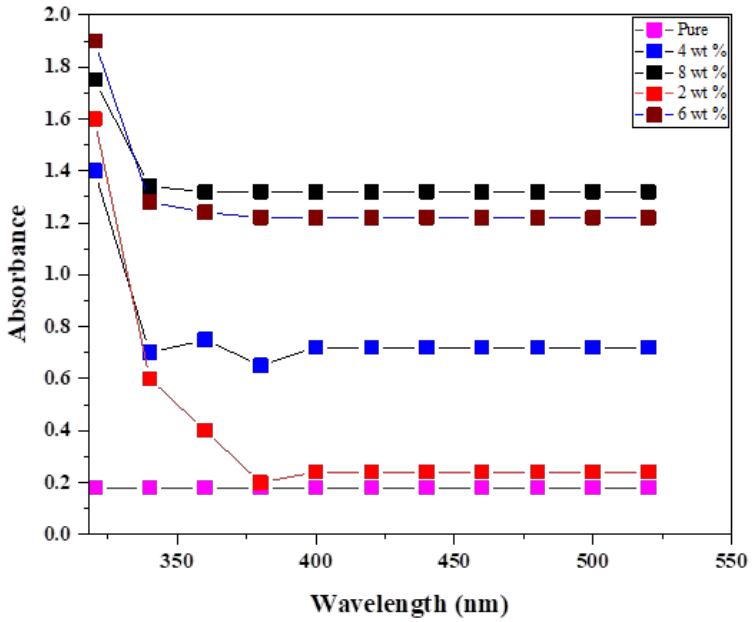

Fig. 3. The wavelength-dependent variation of absorbance for resulting PAN-PEG-TiO_2 nanocomposites.

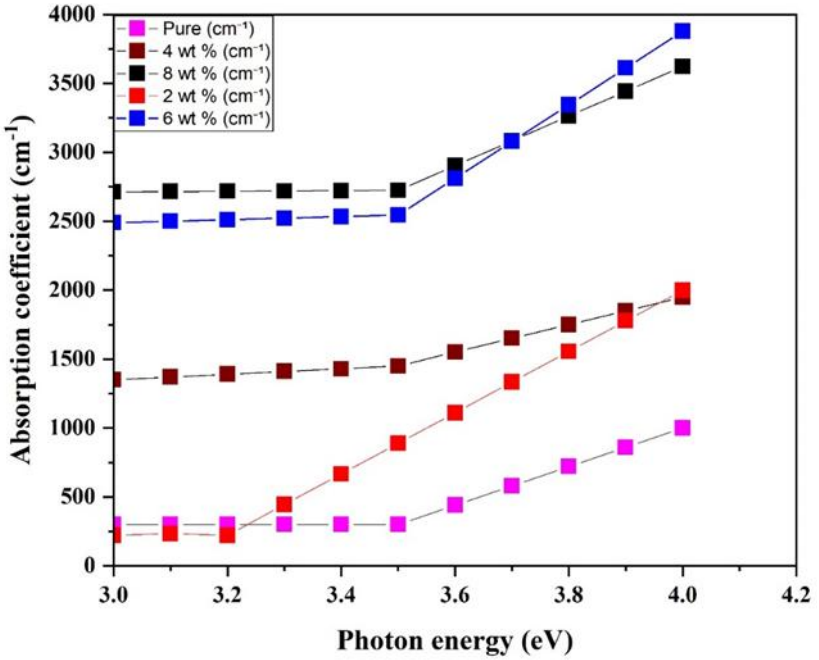

Fig. 4. The photon energy-dependent variation of absorption coefficient (α) for PAN-PEG-TiO_2 nanocomposites.

system (Fig. 1b) after the incorporation of TiO_2 nanoparticles into the polymer matrix show a dramatic transformation in the diffraction pattern as compared to pure polymer systems. The prominent sharp peak at 2θ ≈ 25° corresponds to the (101) crystallographic plane of anatase TiO_2, confirming the successful integration of crystalline TiO_2 nanoparticles within the PAN-PEG polymer matrix while maintaining their anatase phase structure. This pattern is characterized by a significantly elevated and broad background signal, which is attributed to the amorphous and semi-crystalline regions of the PAN-PEG polymer blend [23]. The presence of broad peaks in the 15-35° and 40-60° regions, indicates the semi-crystalline nature of polymer matrix and possible polymer-nanoparticle interactions that affect the local molecular ordering. The high signal-to-noise ratio and the retention of the anatase peak intensity demonstrate excellent dispersion of TiO_2 nanoparticles throughout the polymer matrix without significant agglomeration, while the interaction between the inorganic nanofillers and the organic polymer chains creates a hybrid material structure that combines the crystalline properties of TiO_2 with the flexible characteristics of the PAN-PEG blend, resulting in enhanced optical properties suitable for biological applications [24-28].

This FESEM images in Fig. 2(a, b) demonstrates the successful incorporation and uniform dispersion of TiO_2 nanoparticles within the PAN-PEG polymer matrix [29-31]. The image clearly shows well-dispersed spherical TiO_2 nanoparticles with measured sizes of D1 = 42.81 nm, D2 = 24.78 nm, and D3 = 41.67 nm indicats a relatively narrow size distribution with an average particle size of approximately 35-40 nm. The nanoparticles appear as well-defined spherical components, which are uniformly distributed across the polymer surface without significant agglomeration or clustering. The polymer matrix background shows a textured shape that differs significantly from the smooth morphology of pure PAN-PEG, suggesting strong interfacial interactions between the nanoparticles and polymer chains. This morphological structure is particularly advantageous for biological applications as it provides numerous surface-exposed TiO_2 nanoparticles that can interact with high flexibility of the polymer matrix, ultimately contributing to the enhanced optical properties through increased light scattering, photocatalytic activity, and UV absorption capabilities in direction of biological sensing and antimicrobial applications [27, 28, 32-35].

The absorbance of the PAN-PEG mixture with

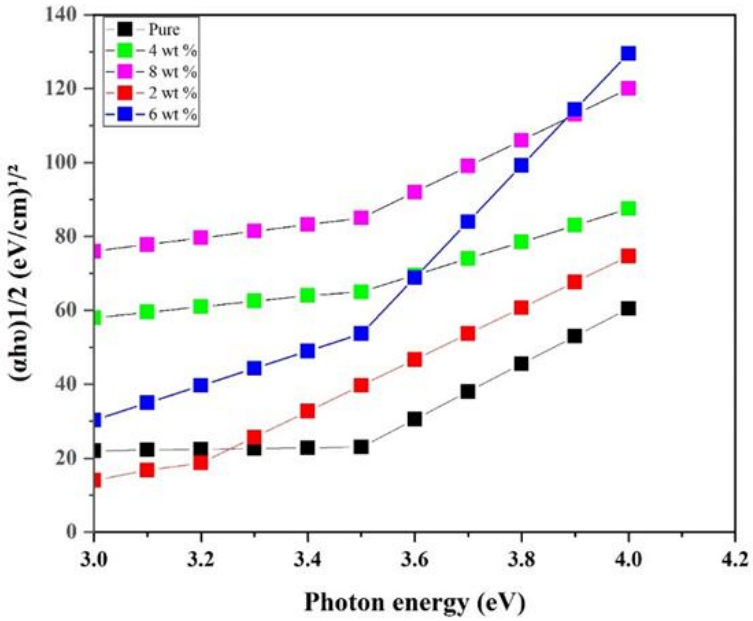

Fig. 5. The photon energy-dependent variation of $(\alpha h\upsilon)^{1/2}$ for PAN-PEG- TiO_2 nanocomposites.

wavelength range of 220-800 nm is affected by the addition of TiO_2 nanoparticles, as displayed in Fig. 3.

When the proportion of TiO_2 nanoparticles is increased, Fig. 4 shows how the absorption coefficient of the PAN-PEG mixture changes with

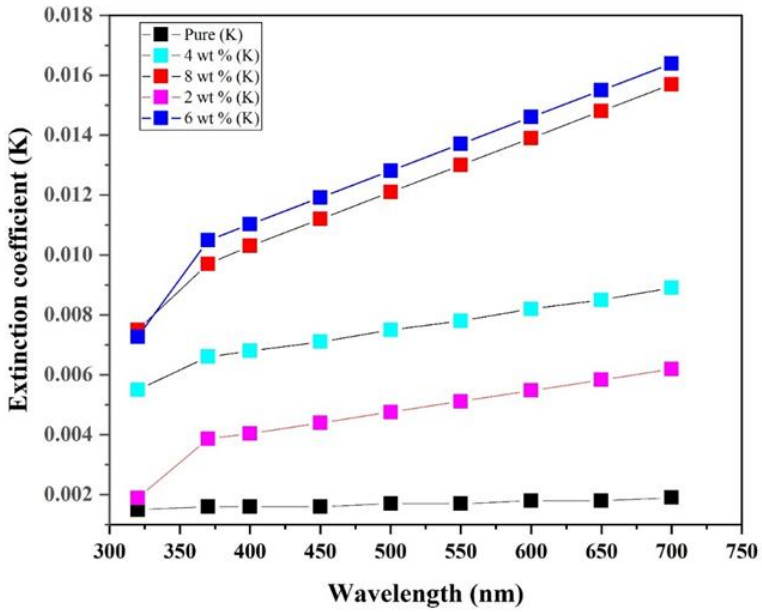

Fig. 6. The wavelength-dependent variation of extinction coefficient for resulting PAN-PEG-TiO_2 nanocomposites.

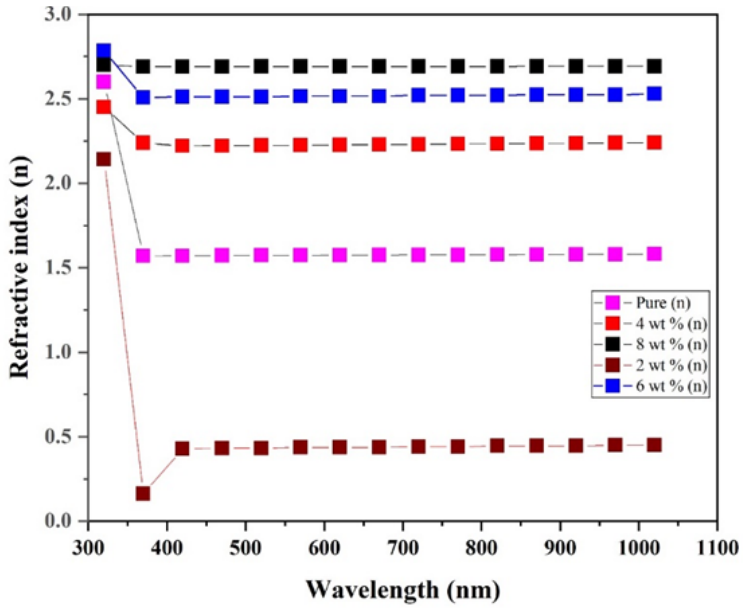

Fig. 7. The wavelength-dependent variation of refractive index for PAN-PEG- TiO_2 nanocomposites.

respect to photon energy. According to the data, the free electrons in the TiO_2 nanoparticles absorb more of the incident radiation, leading to a higher absorption coefficient for the PAN-PEG blend.

An indirect energy gap exists in the nanocomposites when the absorption coefficient of the PAN-PEG-TiO_2 nanocomposites is below 10^4 cm^{-1}. When the concentration of TiO_2

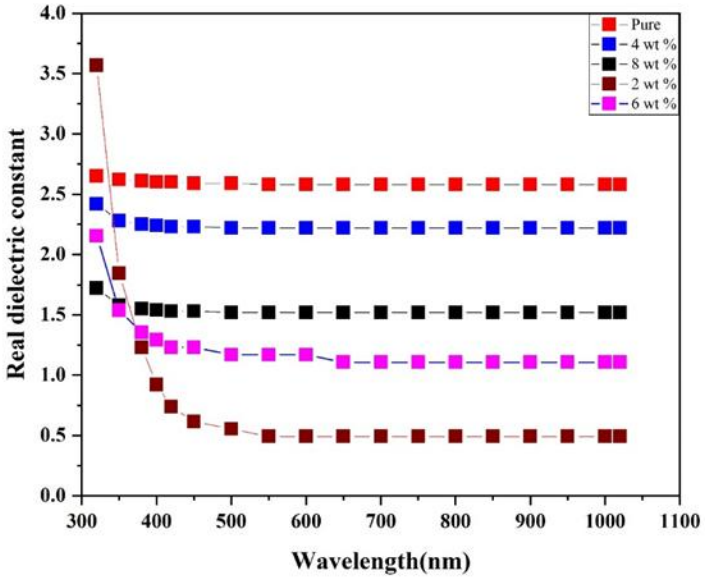

Fig. 8. The wavelength-dependent variation of real part of dielectric constant for PAN-PEG- TiO_2 nanocomposites.

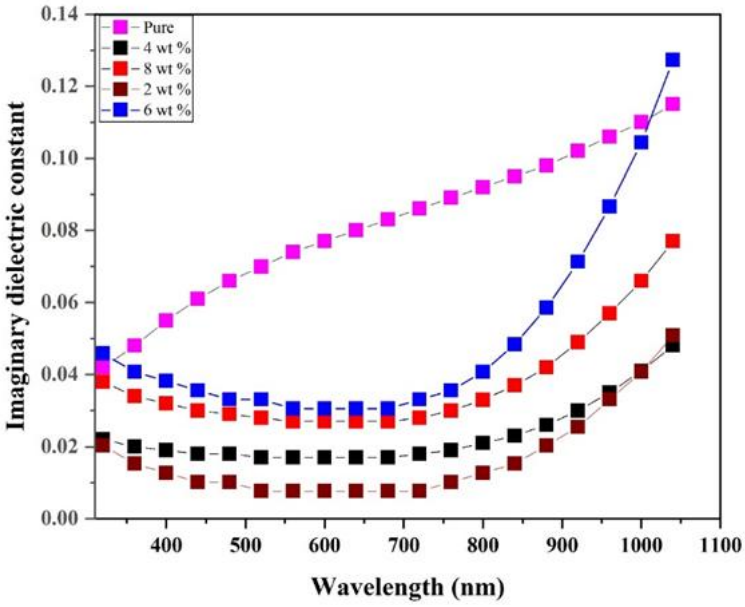

Fig. 9. The wavelength-dependent variation of dielectric constant for PAN-PEG- TiO_2 nanocomposites.

nanoparticles increases, the energy band gap between the indirect permitted and prohibited transitions decreases [19], as shown in Fig. 5. The high conductivity and narrow band gap are a result of electrons graphically transitioning from the valance band to the conduction band on these local levels.

The extinction coefficient of the PAN-PEG mixture changes with concentration of TiO_2 nanoparticles, as shown in Fig. 6. As the concentration of TiO_2 nanoparticles enhances, the extinction coefficient of the blends increases [20].

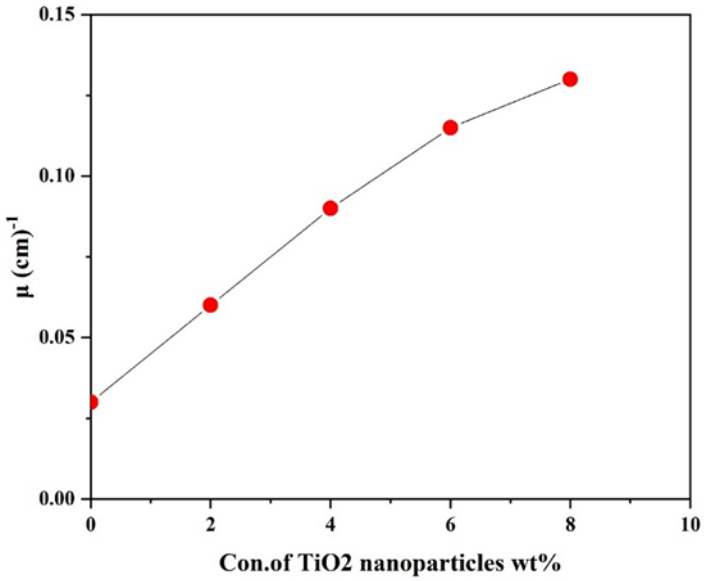

Fig. 10. TiO_2's concentration-dependent variation of N/N_0 for composite.

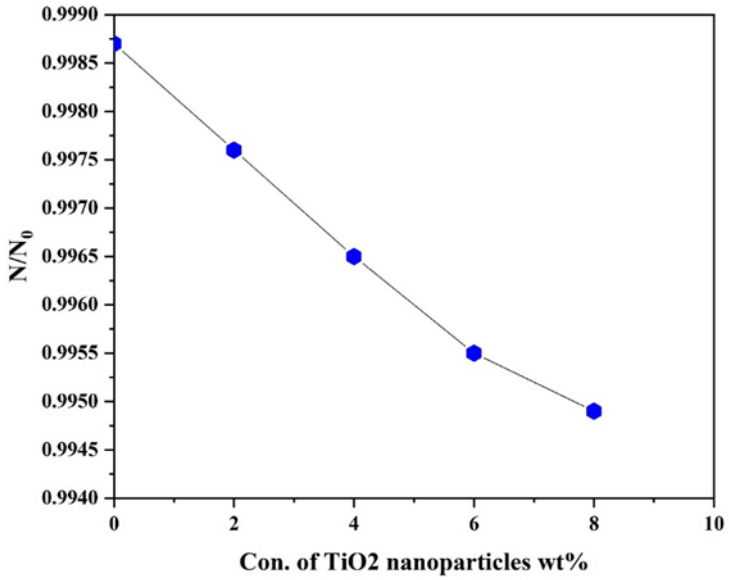

Fig. 11. TiO_2's concentration-dependent variation in attenuation coefficients of gamma radiation for composite.

Fig. 7 displays the relationship between the incident photon energy and the refractive index of a PAN-PEG blend containing diverse concentrations of TiO_2 nanoparticles. Since TiO_2 nanoparticles produce a greater packing density, the refractive index of resulting PAN-PEG-TiO_2 nanocomposites rises as the TiO_2 content increases [20].

The wavelength dependence of the real and imaginary components for the dielectric constant of PAN-PEG-TiO_2 nanocomposites with different concentrations of TiO_2 nanoparticles are depicted in Figs. 8 and 9, respectively. It can be deduced that as the fraction of TiO_2 nanoparticles in PAN-PEG-TiO_2 nanocomposites increases, the material's refractive index (n) and extinction coefficient (k) rises [21].

The calculation of gamma radiation in PAN-PEG-TiO_2 nanocomposites is as follows:

$$N = N_0 \exp(-\mu t) \quad (7)$$

where, N_0 is the number of radiation particles recorded at a specific period, N is the number counted at the same time, with a sample thickness of (d), and μ is attenuation coefficient of gamma radiation for PAN-PEG-TiO_2 nanocomposites [22]. In order to estimate linear attenuation coefficients, the transmitted gamma ray fluxes of PAN-PEG-TiO_2 nanocomposites were measured using the Geiger counter. Figs. 10 and 11 show N/N_0 variation of PAN-PEG-TiO_2 nanocomposites. The rise of the attenuation radiation reduces transmission radiation as weight percentages of TiO_2 nanoparticles increases [36-38].

CONCLUSION

The present investigation showed that the absorbance of the PAN-PEG composite rises with the concentration of TiO_2 nanoparticles. XRD and FESEM analyses demonstrated the successful synthesis of highly crystalline anatase TiO_2 nanoparticles and their excellent dispersion within the PAN-PEG matrix. Results showed that as the concentration of TiO_2 nanoparticles rises, PAN-PEG composite's real and imaginary dielectric constants, extinction coefficient, and absorption coefficient enhances. The energy band gap of the PAN-PEG composite is enhanced by increasing the proportion of TiO_2 nanoparticles. Finally, the Lambda capacity of PAN-PEG-TiO_2 nanocomposites has also been explored. The PAN-PEG-TiO_2 nanocomposites showed improved optical and shielding properties that make them effective for use in applications that involve gamma ray shielding.

CONFLICT OF INTEREST

The authors declare that there is no conflict of interests regarding the publication of this manuscript.

REFERENCES

1. Chen G, Xu Y, Shi T, Wu X, Zhang X, Wen R, et al. Preparation and properties of polyacrylonitrile/polyethylene glycol composite fibers phase change materials by centrifugal spinning. Materials Research Express. 2019;6(9):095502.
2. Adegbola TA, Agboola O, Fayomi OSI. Review of polyacrylonitrile blends and application in manufacturing technology: recycling and environmental impact. Results in Engineering. 2020;7:100144.
3. Abdul-Rida NA, Talib KM. New Chalcone Derivatives as Anticancer and Antioxidant Agents: Synthesis, Molecular Docking Study and Biological Evaluation. Chemical Problems. 2024;22(2):177-186.
4. Hamzah SK, Jabbar NK, Almzaiel AJ, sabit RA. The Role Caspase-8 and DNA Methylation in patients with Ovarian Cancer: Relationship with Oxidative Stress and Inflammation. Research Journal of Pharmacy and Technology. 2021:2676-2680.
5. Sahib IJ, Aljeboree AM, Mahdi AB, Jasim LS, Alkaim AF. Highly efficient removal of toxic Pb(II) from aqueous solution by chitosan-g-p(AA-co-AAm) hydrogel: Kinetic, models. AIP Conference Proceedings: AIP Publishing; 2023. p. 040073.
6. Synthesis, Characterization And Antibacterial Analysis Of Benzocaine Schiff Base Metal Complexes. Nanotechnology Perceptions. 2024;20(6).
7. Nassier LF, Shinen MH. Study of the optical properties of poly (methyl methacrylate) (PMMA) by using spin coating method. Materials Today: Proceedings. 2022;60:1660-1664.
8. Abdullah OG, Saber DR, Hamasalih LO. Complexion Formation in PVA/PEO/$CuCl_2$ Solid Polymer Electrolyte. Universal Journal of Materials Science. 2015;3(1):1-5.
9. Synthesis and Characterization of Zinc(II), Cadmium(II) and Palladium(II) Complexes with the Thiophene-Derived Schiff Base Ligand. American Chemical Society (ACS).
10. Khazaali AFG. Enhanced Adsorption of Malachite Green Using Chitosan-grafted-poly(acrylic acid)/MWCNTs Hydrogel Nanocomposite: Synthesis, Characterization and Kinetic Studies. Chemical Interactions. 2025;1(3):15-20.
11. Jasim LS, Abdulsahib WK, Ganduh SH, Radia ND. New Approach for Sulfadiazine Toxicity Management using Carboxymethyl Cellulose Grafted Acrylamide Hydrogel. International Journal of Drug Delivery Technology. 2020;10(02):259-264.
12. Kareem Hamzah S. Study some biochemical parameters in pregnant women with hypertension. Journal of Physics: Conference Series. 2019;1234(1):012092.
13. Singh S, Maurya IC, Srivastava P, Bahadur L. Synthesis of nanosized TiO_2 using different molecular weight polyethylene glycol (PEG) as capping agent and their

performance as photoanode in dye-sensitized solar cells. J Solid State Electrochem. 2020;24(10):2395-2403.
14. Gaabour LH. Effect of addition of TiO_2 nanoparticles on structural and dielectric properties of polystyrene/polyvinyl chloride polymer blend. AIP Advances. 2021;11(10).
15. Spectrophotometric Determination of Metoclopramide- HCl in the standard raw and it compared with pharmaceuticals. Journal of Pharmaceutical Negative Results. 2021;21(2).
16. Atyaa AI, Radhy ND, Jasim LS. Synthesis and Characterization of Graphene Oxide/Hydrogel Composites and Their Applications to Adsorptive Removal Congo Red from Aqueous Solution. Journal of Physics: Conference Series. 2019;1234(1):012095.
17. Mahmood Taher A, Ali Kadhim Kyhoiesh H, Shakir Waheeb A, Al-Adilee KJ, Jasim LS. Synthesis, characterization, biological activity, and modelling protein docking of divalent, trivalent, and tetravalent metal ion complexes of new azo dye ligand (N,N,O) derived from benzimidazole. Results in Chemistry. 2024;12:101911.
18. Electrical and Optical characterization of Malonic acid doped Poly Vinyl Alcohol polymer electrolytes. International Journal For Innovative Engineering and Management Research. 2021:246-254.
19. Hamdalla TA, Hanafy TA, Bekheet AE. Influence of Erbium Ions on the Optical and Structural Properties of Polyvinyl Alcohol. Journal of Spectroscopy. 2015;2015:1-7.
20. Kadhim K, Agool I, Hashim A. Effect of Zirconium Oxide Nanoparticles on Dielectric Properties of (PVA-PEG-PVP) Blend for Medical Application. Journal of Advanced Physics. 2017;6(2):187-190.
21. Kurt A. Influence of AlCl_3 on the optical properties of new synthesized 3-armed poly(methyl methacrylate) films. Turkish Journal of Chemistry. 2010.
22. Azani A, Halin DSC, Razak KA, Abdullah MMAB, Nabiałek M, Ramli MM, et al. The Effect of Polyethylene Glycol Addition on Wettability and Optical Properties of GO/TiO_2 Thin Film. Materials. 2021;14(16):4564.
23. Nabeel AA-R, Adnan S, Jaber QAH. Development of Novel Imaging Fluorescent Agents Bearing Anti-Inflammatory Drugs: Synthesis, Structural Characterization and Evaluation of Biological Activity. Russian Journal of Bioorganic Chemistry. 2020;46(4):620-626.
24. Jamel HO, Jasim MH, Mahdi MA, Ganduh SH, Batool M, Jasim LS, et al. Adsorption of Rhodamine B dye from solution using 3-((1-(4-((1H-benzo[d]imidazol-2-yl)amino) phenyl)ethylidene)amino)phenol (BIAPEHB)/ P(AA-co-AM) composite. Desalination and Water Treatment. 2025;321:101019.
25. Jasim LS, Aljeboree AM, Sahib IJ, Mahdi MA, Abdulrazzak FH, Alkaim AF. Effective adsorptive removal of riboflavin (RF) over activated carbon. AIP Conference Proceedings: AIP Publishing; 2022. p. 030030.
26. Al-Masoudi NA, Kassim AG, Abdul-Reda NA. Synthesis of Potential Pyrimidine Derivatives via Suzuki Cross-Coupling Reaction as HIV and Kinesin Eg5 Inhibitors. Nucleosides, Nucleotides and Nucleic Acids. 2014;33(3):141-161.
27. Danagody B, Bose N, Rajappan K, Iqbal A, Ramanujam GM, Anilkumar AK. Electrospun PAN/PEG Nanofibrous Membrane Embedded with a MgO/gC_3N_4 Nanocomposite for Effective Bone Regeneration. ACS Biomaterials Science and Engineering. 2023;10(1):468-481.
28. Jo EH, Chang H, Kim SK, Roh KM, Kim J, Jang HD. Pore size-controlled synthesis of PEG-derived porous TiO_2 particles and photovoltaic performance of dye-sensitized solar cells. Mater Lett. 2014;131:244-247.
29. Hiroki A, Taguchi M. Development of Environmentally Friendly Cellulose Derivative-Based Hydrogels for Contact Lenses Using a Radiation Crosslinking Technique. Applied Sciences. 2021;11(19):9168.
30. Mahde BW, Sultan AM, Mahdi MA, Jasim LS. Kinetic Adsorption and Release Study of Sulfadiazine Hydrochloride Drug from Aqueous Solutions on GO/P(AA-AM-MCC) Composite. International Journal of Drug Delivery Technology. 2022;12(04):1583-1589.
31. Mahdi MA, Oroumi G, Samimi F, Dawi EA, Abed MJ, Alzaidy AH, et al. Tailoring the innovative Lu_2CrMnO_6 double perovskite nanostructure as an efficient electrode materials for electrochemical hydrogen storage application. Journal of Energy Storage. 2024;88:111660.
32. Sajeesh S, Sharma CP. Mucoadhesive hydrogel microparticles based on poly (methacrylic acid-vinyl pyrrolidone)-chitosan for oral drug delivery. Drug Deliv. 2010;18(4):227-235.
33. Kianipour S, Razavi FS, Hajizadeh-Oghaz M, Abdulsahib WK, Mahdi MA, Jasim LS, et al. The synthesis of the P/N-type $NdCoO_3$/g-C_3N_4 nano-heterojunction as a high-performance photocatalyst for the enhanced photocatalytic degradation of pollutants under visible-light irradiation. Arabian Journal of Chemistry. 2022;15(6):103840.
34. Hosseini M, Ghanbari M, Dawi EA, Mahdi MA, Ganduh SH, Jasim LS, et al. Investigations of nickel silicate for degradation of water-soluble organic pollutants. Int J Hydrogen Energy. 2024;61:307-315.
35. Batool M, Haider MN, Javed T. Applications of Spectroscopic Techniques for Characterization of Polymer Nanocomposite: A Review. Journal of Inorganic and Organometallic Polymers and Materials. 2022;32(12):4478-4503.
36. Halpern J, Crane HR. The Absorption Coefficient of 5.8-Mev Gamma-Radiation in Aluminum. Phys Rev. 1939;55(3):258-259.
37. Radia ND, Alshamusi QKM, Sahib IJ, Jasim LS, Aljeboree AM, Alkaim AF. Oxidative coupling of phenylephrine hydrochloride using N,N-dimethyl-p-phenylenediamine: Stability and higher sensitivity. AIP Conference Proceedings: AIP Publishing; 2022. p. 030026.
38. Jabir FA, Hamzah SK. SOX17 and RASSAF1A promoters methylation in circulation tumor cell and cell free DNA isolated from plasma in breast cancer Iraqi women patients. Research Journal of Pharmacy and Technology. 2018;11(5):2000.